Global Change Biology (2003) **9,** 510–524

Changes in carbon storage and fluxes in a chronosequence of ponderosa pine

B. E. LAW*, O. J. SUN*, J. CAMPBELL*, S. VAN TUYL* and P. E. THORNTON†
College of Forestry, Oregon State University, Corvallis, OR 97331-5752, USA, †Climate and Global Dynamics Division, National Center for Atmospheric Research, Boulder, CO 80305, USA

Abstract

Forest development following stand-replacing disturbance influences a variety of ecosystem processes including carbon exchange with the atmosphere. On a series of ponderosa pine (*Pinius ponderosa* var. Laws.) stands ranging from 9 to > 300 years in central Oregon, USA, we used biological measurements to estimate carbon storage in vegetation and soil pools, net primary productivity (NPP) and net ecosystem productivity (NEP) to examine variation with stand age. Measurements were made on plots representing four age classes with three replications: initiation (*I*, 9–23 years), young (*Y*, 56–89 years), mature (*M*, 95–106 years), and old (*O*, 190–316 years) stands typical of the forest type in the region. Net ecosystem productivity was lowest in the *I* stands ($-124\,g\,C\,m^{-2}\,yr^{-1}$), moderate in *Y* stands ($118\,g\,C\,m^{-2}\,yr^{-1}$), highest in *M* stands ($170\,g\,C\,m^{-2}\,yr^{-1}$), and low in the *O* stands ($35\,g\,C\,m^{-2}\,yr^{-1}$). Net primary productivity followed similar trends, but did not decline as much in the *O* stands. The ratio of fine root to foliage carbon was highest in the *I* stands, which is likely necessary for establishment in the semiarid environment, where forests are subject to drought during the growing season (300–800 mm precipitation per year). Carbon storage in live mass was the highest in the *O* stands (mean $17.6\,kg\,C\,m^{-2}$). Total ecosystem carbon storage and the fraction of ecosystem carbon in aboveground wood mass increased rapidly until 150–200 years, and did not decline in older stands. Forest inventory data on 950 ponderosa pine plots in Oregon show that the greatest proportion of plots exist in stands ~100 years old, indicating that a majority of stands are approaching maximum carbon storage and net carbon uptake. Our data suggests that NEP averages $\sim 70\,g\,C\,m^{-2}\,year^{-1}$ for ponderosa pine forests in Oregon. About 85% of the total carbon storage in biomass on the survey plots exists in stands greater than 100 years, which has implications for managing forests for carbon sequestration. To investigate variation in carbon storage and fluxes with disturbance, simulation with process models requires a dynamic parameterization for biomass allocation that depends on stand age, and should include a representation of competition between multiple plant functional types for space, water, and nutrients.

Keywords: biomass, carbon cycle, carbon sequestration, forest development, net ecosystem productivity, net primary productivity, Oregon, *Pinus ponderosa*, soil carbon

Revised version received 1 January 2003

Introduction

Disturbance to terrestrial ecosystems by human activity indisputably impacts the global terrestrial C balance (IPCC, 2001). Land management and land use change affect vegetation cover, microclimate, and soil processes. In forests, primary modes of disturbance are wildfire and underburning, logging, windthrow, and insects and diseases. Litter removal through frequent underburning or 'raking' to remove wildfire fuels can reduce litter mass and quality, and subsequently nutrient availability to trees and stand productivity (Monleon *et al*., 1997). The effect of logging on carbon storage and fluxes depends on the amount of biomass removed from a site, the amount and quality of debris left on-site to decompose, soil fertility, and productivity of the regrowth. Large amounts of

Correspondence: Beverly E. Law, 328 Richardson Hall, College of Forestry, Oregon State University, Corvallis, OR 97331-5752, USA, e-mail: bev.law@oregonstate.edu

woody detritus left on-site after logging may result in a relatively large amount of heterotrophic respiration for years to decades depending on decomposition rates.

Within a forest type, mean annual fluxes of carbon dioxide to the atmosphere are strongly influenced by the time since stand replacing disturbance (Cohen *et al*., 1996; Law *et al*., 2001b), whereas interannual variation in the net carbon uptake (NEE or NEP) is likely driven by the effect of year-to-year variation of climate on short-term carbon pools (foliage, soil microbes) through variation in photosynthesis and respiration by autotrophs and heterotrophs (Schimel *et al*., 2001). Our sapflow and predawn water potential measurements at young and old ponderosa pine flux sites showed that the young trees suffered more drought stress than the mature and old trees, likely because their roots could not access deep soil water (Irvine *et al*., 2002). Drought stress in young trees appears to slow reestablishment; young pine stands in this region can take 10–20 years to reestablish, and for carbon uptake to exceed carbon losses through respiration (Law *et al*., 2001a). Similarly, Amiro (2001) and Litvak *et al*. (2003) suggested that carbon uptake offset losses between 10 and 20 years following disturbances from fire and harvest in boreal forests where unfavourable environmental conditions limit growth.

In this paper, we use biological measurements in a chronosequence of ponderosa pine (*Pinus ponderosa* var. Laws.) forests in central Oregon, USA, to quantify carbon storage and annual fluxes associated with stand developmental stage, and explore the implications to the current age-distribution of ponderosa pine in Oregon. We hypothesize that, in ponderosa pine forests, carbon storage in live mass does not decrease significantly from mature to old stands, and that the old stands, on average, are not 'carbon neutral'. In addition, we hypothesize that heterotrophic respiration is primarily from soils in this semiarid system, where decomposition of woody detritus is relatively slow. We also simulate the historical patterns of disturbance and recovery at each of the chronosequence sites with the process model, Biome-BGC, and test the need for dynamic parameterization of some variables. We explore the variability in disturbance recovery responses related to atmospheric CO_2 concentration during recovery. This paper builds on earlier flux studies and carbon budget estimates at the young and old Metolius flux sites (Law *et al*., 2001b).

Methods and materials

Study sites

In 12 ponderosa pine stands ranging from 9 to > 300 years, we measured live and dead carbon pool and net primary productivity (NPP) to estimate annual net ecosystem productivity (NEP). All 12 plots were located within a 100-km^2 area in the Metolius River basin of central Oregon. Three of the stands are the Metolius AmeriFlux sites, where micrometeorological and automated soil chamber measurements have been made. This is a semiarid region where most of the precipitation occurs between October and June, and the winters are cool. Annual rainfall averages 300–800 mm and the 30-years mean is 550 mm, with 1–2% of the total occurring in the summer.

The 12 stands represent four age classes replicated three times including initiation (*I*, stand age 9–20 years), young (*Y*, 56–89 years), mature (*M*, 95–106 years), and old (*O*, 190–316 years). Stands were selected to be representative of their age-class for the region. Stand age was determined from the mean age of the oldest 10% of trees cored on each plot. Ponderosa pine dominates the overstorey in all 12 plots with varying amounts of grand fir (*Abies grandis*), western larch (*Larix occidentalis*), and incense cedar (*Calocedrus decurrens*) occurring in some stands. The understorey includes manzanita (*Arctostaphylos patula*) and bitterbrush (*Purshia tridentata*), and is more conspicuous in younger stands. The soil is generally sandy loam. Historical records indicate that logging rather than wildfire had been the source of stand-replacing disturbance in all but the *O* stands in our study (USDA Forest Service, Sisters Ranger District). The catastrophic fires of 1911 came close to two of the stands, and one of the old stands had been underburned in 1990. Site characteristics are summarized in Table 1.

Environmental measurements

Carbon dioxide, water vapour, and energy fluxes were estimated from micrometeorological measurements using the eddy covariance technique at old (*OS*) and initiation stage (*YS*) flux sites in 2000 (Law *et al*., 2001b; Anthoni *et al*., 2002). Flux systems were comprised of three-axis sonic anemometers that measured wind speed and virtual temperature (Solent model 1012 R2, Gill instruments, Lymington, England; CSAT-3 Campbell Scientific, Inc., Utah), open-path infrared gas analyzers that measured concentrations of water vapour and CO_2 (LI-7500, LI-COR, Lincoln, NE), and a suite of software data processing. Fluxes were averaged half-hourly, and the records in the database were evaluated for data quality. Details on the instrumentation, flux correction methods and calculations were reported in Anthoni *et al*. (2002). The flux data were used to compare weekly estimates of net ecosystem production (NEP) by the two flux sites.

Half-hourly measurements of climatic variables made at the top of the flux towers included air temperature (T_{air}), vapour pressure deficit (*D*), incident photosynthetically active radiation (PAR), and rainfall. Soil moisture

Table 1 Characteristics of ponderosa pine stands in the Metolius area of central Oregon

Plot ID	Longitude	Latitude	Altitude (m)	Stand density (#Trees ha^{-1})	Mean* DBH(cm)	Mean* Height(m)	Stump density (#Pieces ha^{-1}), mean diameter†	Species composition	Stand age, class‡	History
25§	−121.568	44.437	1165	431	11.3 (0.49, 78)	4.3 (0.16, 78)	204, 41.6 (24.4, 37)	Pipo	23, *I*	Clearcut 1978, natural regeneration, thinned
26	−121.691	44.451	918	272	8.0 (0.48, 77)	2.0 (0.12, 77)	219, 57.0 (21.9, 62)	Pipo, Pico	9, *I*	Clearcut, natural regeneration, no thinning with the current crop, 0.25 mile from polygon of 1911 fire
27	−121.610	44.433	1113	241	9.6 (0.37, 68)	3.8 (0.11, 68)	134, 38.3 (26.6, 38)	Pipo	16, *I*	Clearcut, then thinned 1998, natural regeneration
28	−121.585	44.428	1129	349	21.0 (1.08, 74)	8.3 (0.37, 74)	94, 23.7 (14.5, 20)	Pipo	69, *Y*	Clearcut, natural regeneration, thinned
29	−121.587	44.437	1153	237	30.7 (1.16, 67)	14.5 (0.53, 67)	332, 19.5 (12.0, 94)	Pipo, Cade	56, *Y*	Clearcut, natural regeneration (high shrub density), thinned
30¶	−121.558	44.451	1232	325	29.0 (1.31, 69)	14.0 (0.59, 69)	268, 22.9 (13.3, 57)	Pipo, Cade	89, *Y*	Clearcut, natural regeneration, thinned
31	−121.670	44.434	906	581	27.5 (1.26, 73)	18.9 (0.75, 73)	217, 22.1 (21.1, 46)	Pipo	106, *M*	Clearcut, shallow water table, thinned, 0.5 mile from polygon of 1911 fire
32	−121.669	44.453	899	1281	15.4 (0.82, 68)	10.2(0.46, 68)	0	Pipo, Abgr	93, *M*	Clearcut
33	−121.663	44.463	891	1070	19.0 (1.53, 86)	13.5 (0.93, 86)	87, 28.3 (20.2, 7)	Pipo, Laoc, Abgr	96, *M*	Clearcut, natural regeneration
34**	−121.625	44.498	895	46 526	73.8 (6.37, 7), 14.7 (1.12, 80)	38.9 (1.48, 7), 13.5 (1.05, 80)	0	Pipo	190, *O*	Two layer canopy
35	−121.624	44.501	887	116	55.0 (3.36, 42)	32.6 (1.45, 42)	6, 79.5 (31.8, 2)	Pipo	251, *O*	Underburned 1990, single layer canopy
36	−121.607	44.422	1129	103 628	56.5 (4.90, 13), 9.0 (0.90, 79)	28.9 (1.64, 7), 8.9 (1.05, 79)	56, 64.0 (35.1, 7)	Pipo, Cade	316, *O*	Two layer canopy

Species codes: Abgr, *Abies grandis*; Cade, *Calocedrus decurrens*; Laoc, *Larix occidentalis*; Pico, *Pinus contorta*; Pipo, *Pinus ponderosa*; Psme, *Pseudotsuga menziesii.*

*Values in parentheses are standard errors (SE) and sample size (*n*), i.e. (SE, *n*).

†Diameter at the stump height.

‡The mean age of the oldest 10% of trees in the stand, and age class of stand (*I*, initiation; *Y*, young; *M*, mature; *O*, old).

§*YS* flux site (initiation stand).

¶*IS* flux site (young stand).

***OS* flux site (old-growth stand).

was measure at 0–30 cm depth (CS615s, Campbell Scientific, Logan, UT) and soil temperature at 15 cm depth (Table 2). The continuous meteorological measurements were used in Biome-BGC simulations.

Carbon budgets from biological measurements

In 2001, we measured tree and shrub dimensions, age and growth increment from wood cores, leaf area index (LAI), herbaceous plant biomass, coarse and fine woody detritus, forest floor fine litter mass, soil bulk density, soil C and N concentrations, fine litterfall. On four 10 m radius subplots within each $100 \times 100\,m^2$ plot, structure measurements were made of tree height with a laser ranging scope (MapStar and Impulse 200, Laser Tech, Inc., Englewood, CO), and diameter at breast height (DBH, 1.37 m) on all trees >5 cm DBH. The smaller trees were included in the shrub survey. Increment cores were taken from five trees per subplot in five evenly spaced directions from the subplot centre starting from the north for a total of 20 cores per plot to determine 10-year mean growth increment, age, and wood density. Shrub dimensions (length, width, height, diameter at shrub base) and herbaceous plant biomass were measured on 1–2 m radius microplots at each subplot centre in all stands. In the *I* stands, dimensions were measured on all trees (height, diameter at tree base, base of crown, and DBH), and shrubs on the subplots.

Aboveground biomass, coarse root mass, and 10-year mean productivity of both were estimated from the increment cores and tree dimensions, and local allometric equations. The allometric equations for trees and shrubs were developed in four of the stands (Law *et al*., 2001b). Foliage productivity was calculated from leaf mass per needle age class (LMA) and optical estimates of LAI corrected for clumping and wood interception (LAI-2000, LICOR, Lincoln, NE, USA; methods in Law *et al*., 2001b, 2001c). Fine root turnover rate was assumed to be $0.60\,yr^{-1}$ based on minirhizotron measurements on two plots (Law *et al*., 2001b) and fine root production was calculated for each plot as fine root mass multiplied by fine root turnover.

Carbon storage was determined on live and dead fine (<2 mm diameter) and small coarse roots (2–20 mm). On three plots at the flux sites representing *I*, *Y*, and *O* stands, we collected 18 soil cores (six cores per subplot on three subplots), sampling 0–20 cm, 20–50 cm, and 50–100 cm depths in late April 2001. The sampling was repeated with nine cores on each of those three plots in October. Statistical analysis showed no significant difference in values between the two sampling periods, so we pooled the measurements from the two periods to obtain plot average carbon storage in fine and small coarse roots. For the remaining nine plots, we collected six soil cores to 30 cm depth on each plot in late April and early August. The soil core root mass of the surface 30 cm were scaled to 1 m depth assuming 80% of total mass, as observed in the 1 m profiles. Again, statistical analysis showed no significant difference in the values for the two periods, and data were pooled to obtain plot averages.

Carbon storage in soil was determined from the 12 soil cores used for fine root mass, plus samples to 100 cm depths below those cores. Live vegetation and roots were removed, and the total C and N were determined (LECO CNS2000 analyzer), as well as bulk density and

Table 2 Annual and seasonal climate at the *OS* and *YS* ponderosa pine flux sites, and means for four age classes replicated three times in year 2001

	OS flux site	*YS* flux site	Initiation stands	Young stands	Mature stands	Old stands
Annual mean T_{soil} (°C) at 15 cm depth	7.6 (5.90)	8.5 (6.30)	9.75 (0.85)	8.48 (1.10)	8.74 (1.54)	9.12 (0.57)
Summer mean T_{soil} (°C) at 15 cm depth	15.3 (1.79)	18.8 (2.24)	17.18 (0.20)	16.08 (1.74)	15.51 (1.26)	16.87 (1.44)
Winter maximum soil water content ($m^3\,m^{-3}$; 0–30 cm depth)	0.21 (0.012)	0.22 (0.017)	0.22 (0.02)	0.21 (0.06)	0.14 (0.01)	0.17 (0.02)
Summer minimum soil water content ($m^3\,m^{-3}$; 0–30 cm depth)	0.07 (0.008)	0.06 (0.009)	0.09 (0.01)	0.06 (0.02)	0.08 (0.01)	0.07 (0.01)
Annual mean T_{air} (°C)	8.7 (9.04)	7.9 (8.73)				
Summer mean T_{air} (°C)	18.0 (6.69)	17.4 (5.85)				
Annual diurnal T_{air} amplitude (°C)	10.4 (1.46)	7.5 (1.20)				
Summer diurnal T_{air} amplitude (°C)	15.1 (0.77)	12.0 (0.66)				
Annual rain (mm)	444	476				
Summer rain (mm)	34	44				
Annual PAR ($MJ\,m^{-2}$)	2287	2211				

Summer is defined as June through September. Standard deviations are shown in parentheses.

soil texture (hydrometer method, Central Analytical Laboratory, Oregon State University). Soil carbon content was calculated for each soil layer from layer depth, bulk density adjusted for the volume of coarse fraction (> 2 mm), and percent organic carbon data, and summed for all layers to estimate total soil carbon content to 1 m depth.

Coarse woody debris (CWD > 10 cm diameter, and > 1 m length) and fine woody debris (FWD 1–10 cm diameter) mass were measured following Harmon & Sexton (1996). Downed CWD (logs) were measured on four 75 m line transects on each plot and the species and decay class of each piece were identified (5 classes). Dimensions of standing dead trees (snags and stumps) were used in the allometric equations to determine standing dead volume. Fine woody debris was measured on four 15 m transects per subplot for all four subplots. We calculated C mass in CWD and FWD from estimates of wood volume for each species and decay class and corresponding wood density of partially decayed woody detritus (Harmon & Sexton, 1996; M. Harmon, pers. comm.). The annual loss of carbon from CWD (R_{hCWD}) and FWD (R_{hFWD}) decomposition was calculated from mass per m^2 ground, and species–specific decomposition rates for the area (M. Harmon, pers. comm.; Harmon *et al*., 1990).

We computed NEP from measurements of carbon fluxes by the major pools. Net ecosystem production is gross photosynthesis (GPP) minus autotrophic (R_a) and heterotrophic respiration. The mass balance approach for estimating NEP begins with separation of above and belowground fluxes (Eqn (1)).

$$\mathrm{NEP} = (\mathrm{NPP_A} - R_{\mathrm{hWD}}) + (\mathrm{TBCA} - R_S) \quad (1)$$

where NPP_A is aboveground net primary production (sum of wood and foliage, over- and understorey plants), R_{hWD} is the respiration from woody debris (decomposition of coarse and fine woody debris, stumps and snags), TBCA is total belowground carbon allocation, and R_S is total soil surface CO_2 flux. Following Raich & Nadelhoffer (1989), TBCA can be determined by subtracting annual litterfall carbon from R_S plus any detectable changes in belowground C pools (Eqn (2)). By substituting the TBCA equation into Eqn (1), R_S cancels, allowing NEP to be calculated according to Eqn (3), where ΔC_{FR} and ΔC_{CR} are the changes in fine and coarse root carbon with stand age, ΔC_S is the net change in mineral soil C, and ΔC_L is annual litterfall carbon. Coarse root carbon was calculated as the difference between the net growth of live coarse roots and the decomposition of coarse roots attached to snags and stumps. The change in C stored in roots, litter and soil with stand age accounted for non-steady state conditions when using a carbon balance approach to estimating TBCA (Giardina & Ryan, 2002). Measurements of fine root mass and soil C were not significantly different across the 300 years chronosequence, consequently ΔC_{FR} and ΔC_S were assumed to be zero.

$$\mathrm{TBCA} = R_S - \Delta C_L + \Delta C_{FR} + \Delta C_{CR} + \Delta C_S \quad (2)$$

$$\mathrm{NEP} = (\mathrm{NPP_A} - R_{\mathrm{hWD}}) + (\Delta C_{FR} + \Delta C_{CR} + \Delta C_S - \Delta C_L) \quad (3)$$

The remaining carbon fluxes, belowground net primary production (NPP_B), total heterotrophic respiration (R_h), and heterotrophic respiration from soil (R_{hS}), were calculated using Eqns (4), (5), and (6), respectively.

$$\mathrm{NPP_B} = (\mathrm{NPP_{CR}}) + (\mathrm{NPP_{FR}}) \quad (4)$$

$$R_h = \mathrm{NEP} - (\mathrm{NPP_A} + \mathrm{NPP_B}) \quad (5)$$

$$R_{hS} = R_h - (R_{hWD}) \quad (6)$$

Uncertainty estimates were made for each component used for computing NEP by defining upper and lower boundaries based on various estimates of component error. Error estimates in NPP_A and ΔC_{CR} are based on error in radial growth estimates propagated through the allometric models. Uncertainties in litterfall and soil carbon estimates were identified as within plot sample standard deviations. Maximum boundaries for potential ΔC_{FR} and ΔC_S were assigned to plots in each age class based on a maximum range of pool values between age classes. Uncertainty in CWD and FWD is based on estimates of uncertainty in the sampling methodology (J. Sexton, Oregon State University, pers. comm.). A Monte Carlo model was then used to estimate means and uncertainties in NEP (uncertainties expressed as ± 1 SD of 1000 Monte Carlo iterations; Law *et al*., 2001b).

Physiological measurements

We measured assimilation rates in relation to intercellular CO_2 concentration (A–C_i curves) on 1-year-old-needles at mid-canopy of 15- and 50-year-old-trees at two of the chronosequence sites (plots 25 and 34) using a portable infrared gas analyzer (LI-6400; LI-COR, Lincoln, NE, USA). Measurements were made in June and August. Foliar carbon and nitrogen (LECO CNS2000 analyzer), and specific leaf area (SLA; m^2 one-sided leaf area g^{-1} dry mass) were determined on the same needles collected immediately after photosynthesis measurements. These data were necessary for calculating Biome-BGC model parameters. We follow the methods of Wilson *et al*. (2000) and Thornton *et al*. (2002; their Appendix A) to estimate leaf nitrogen in the Rubisco enzyme (*flnr*) from variables derived from A–C_i curves,

given concurrent measurements of leaf temperature, SLA, and foliar C : N. In this analysis we assume that the specific activity of Rubisco (*act*) varies only with temperature ($60\,\mu mol\,g^{-1}$ Rubisco s^{-1} at 25 °C, from Woodrow & Berry, 1988), and that the mass fraction of nitrogen in the Rubisco molecule is constant (0.1397, calculated from amino acid composition of Rubisco given in Kuehn & McFadden, 1969).

Data analysis

The effects of stand development (stand age classes) on various carbon pools and carbon fluxes were examined by performing one-way analysis of variance using the ANOVA procedure of SAS (Version 8; SAS Institute Inc., 1999) based on our experimental design of four age classes with three replications. If the effect of stand age classes were significant on a variable, means were further compared by Duncan's multiple range tests with a confidence level of $P < 0.05$. Non-linear curves of various carbon pools and carbon fluxes as function of stand age were fitted using the built-in statistical program of SigmaPlot (Version 8.0, SPSS Science, IL, USA).

Modeling

We used a daily time step model of coupled carbon, nitrogen, and water cycles (Biome-BGC, version 4.1.1, Thornton *et al*., 2002; with modifications as noted below) to simulate the historical patterns of disturbance and recovery at each of the chronosequence sites. Daily surface weather drivers for the period 1980–1997 from the Daymet database (www.daymet.org, Thornton *et al*., 1997; Thornton & Running, 1999; Thornton *et al*., 2000) were used to drive the model, repeating the sequence as necessary to obtain a weather record of the required length for each site. We followed the simulation ensembling and disturbance simulation methods described in Thornton *et al*. (2002) to isolate the disturbance recovery signal from variability driven by interannual climate fluctuations. We followed the age-class ensembling methods described in Law *et al*. (2001b) to represent mixed age class stands (plots 34 and 36).

The default model parameterization uses static allocation ratios to relate new growth in fine root and woody tissue to new growth of leaves (Thornton *et al*., 2002). An earlier study demonstrated the effects on modeled NEP of changes in these ratios as a function of stand age (Law *et al*., 2001b). With the observations from the current study we were able to construct simple relationships describing the variation of these allocation parameters with stand age, and we tested the hypothesis that this variation reduces model bias in both storage and flux variable comparisons to observations. We used these model results to develop an additional hypothesis regarding variation in leaf nitrogen allocation to the Rubisco enzyme as a function of time since disturbance. We also explored the variability in disturbance recovery responses related to atmospheric CO_2 concentration during recovery. The complete computer code and instructions for running the model to reproduce the results in this manuscript are available from P. E. Thornton on request.

Results and discussion

Air temperature averaged 8 °C in 2001 at the flux sites (Table 2). The summer maximum soil temperature was greatest in the more open *I* stands averaging 20.9 °C at 15 cm depth, and 17.5 °C in the *M* stands with higher leaf area. Soil water content over 0–30 cm depth reached a maximum of $0.22\,m^3\,m^{-3}$ in the winter months for the *I* stands and $0.14\,m^3\,m^{-3}$ for the *M* stands, which on average had the highest leaf area (Table 3). In the summer months, soil water content was similar between sites, reaching a mean low value of $0.08\,m^3\,m^{-3}$.

The *YS* flux site (plot 25 of *I* stands), with half the leaf area of the *OS* flux site (plot 34 of *O* stands) suffered more drought stress during the growing season than the *O* stand, and had consistently lower gross ecosystem productivity (GEP) and less net carbon uptake through the year, and lower annual NPP (Table 4). Weekly NEP(*YS*) average ~20% less than NEP(*OS*) through the year in 2000 (Fig. 1), with the greatest differences in summer (e.g. 40 and $30\,g\,C\,m^{-2}\,week^{-1}$ at *OS* and *YS*). A study on hydraulic redistribution of water suggested that the old trees with more developed root systems were able to access deep soil water during drought (Brooks *et al*., 2002).

Available soil moisture, particularly in spring and early summer, is critical to survival of ponderosa pine seedlings (Barrett, 1979). Competition for water is greatest in the 0–20 cm soil zone (Riegel *et al*., 1992), within which the pines will root in the first year. The process of stand development is function of shade intolerance, conditions favorable for seedling establishment associated with years of above-average precipitation, and frequent fire (Cooper, 1960). Gaps created by mortality allow seedlings to become established when good seed crop years coincide with above-average precipitation. This may explain the slow reestablishment following logging (~8 year difference between logging date and mean stand age in the initiation stands), and combined with logging intensity and the catastrophic fires that occurred in 1911 across the Pacific Northwest, it may explain the high frequency of stands in the 90–130 age classes on private and public lands (Fig. 2).

Table 3 Carbon pools of ponderosa pine stands in the Metolius area of central Oregon

Plot ID	Overstorey LAI*	Understorey LAI*	Total LAI*	LM_A†	LM_B‡	CWD C§	FWD C¶	Fine litter C**	Soil C††	Ecosystem C‡‡
25	0.89 (0.10)	0.57	1.46 (0.15)	802	633	587	459	1696 (698)	6918 (388)[1]	11 513
26	0.14 (0.02)	0	0.14 (0.02)	687	109	1568	1115	1153 (552)	12 686 (1912)	16 899
27	0.29 (0.07)	0.25	0.54 (0.10)	389	215	587	450	841 (271)	5380 (961)	7861
28	1.46 (0.12)	0.39	1.85 (0.13)	3653	1063	404	186	735 (185)	4060 (675)	10 102
29	1.53 (0.11)	0.4	1.93 (0.13)	5261	1816	320	373	1101 (217)	7634 (1617)	16 506
30	2.96 (0.12)	0.16	3.12 (0.12)	6898	2315	1459	382	1147 (310)	7868 (326)[1]	20 069
31	2.18 (0.14)	0.09	2.28 (0.13)	10 806	3489	510	339	1800 (561)	9699 (835)	26 643
32	2.47 (0.10)	0.01	2.48 (0.10)	5459	1603	3801	187	2073 (676)	6906 (590)	20 019
33	3.48 (0.11)	0.2	3.69 (0.12)	14 254	4662	1366	433	2070 (805)	7361 (801)	30 147
34	1.99 (0.14)	0	2.00 (0.12)	12 228	3990	524	451	1127 (348)	5556 (317)[1]	23 875
35	1.83 (0.07)	0.04	1.86 (0.09)	12 326	3829	510	136	1195 (471)	4122 (905)	22 117
36	2.12 (0.14)	0.39	2.50 (0.14)	15707	4837	1177	202	1954 (370)	6496 (2155)	30 372

Values are in grams carbon per m^2 ground basis unless indicated otherwise. Standard deviations are shown in parentheses.
*LAI calculated as m^2 half-surface area foliage per m^2 ground, and corrected for clumping and wood interception; standard errors were computed from grid-point measurements at 39 locations on each plot.
†LM_A is aboveground live mass, including understorey woody and herbaceous plants.
‡LM_B is belowground live mass.
§Coarse woody debris.
¶Fine woody debris.
**Forest floor fine litters, $n = 6$.
††Soil carbon to 1 m depth; $n = 12$, otherwise [1]$n = 18$.
‡‡Ecosystem carbon is the sum of live and dead carbon pools and soil carbon.

Table 4 Annual carbon fluxes of ponderosa pine stands in the Metolius area of central Oregon

Plot ID	Age class*	NPP_A	NPP_B	R_{hS}	R_{hCWD}	R_{hFWD}	ΔC_{CR}	ΔC_{FR}	ΔC_S	NEP
25	*I*	158 (49)	150 (37)	368 (64)	7 (2)	16 (5)	20 (4)	0 (2)	0 (97)	−83 (17)
26	*I*	109 (53)	45 (23)	299 (69)	56 (14)	43 (11)	17 (2)	0 (2)	0 (97)	−244 (29)
27	*I*	75 (22)	87 (75)	173 (79)	16 (4)	18 (5)	15 (2)	0 (2)	0 (97)	−44 (6)
28	*Y*	251 (45)	119 (39)	179 (66)	6 (2)	7 (2)	49 (9)	0 (5)	0 (129)	177 (28)
29	*Y*	200 (34)	175 (54)	294 (72)	8 (2)	14 (4)	45 (9)	0 (5)	0 (129)	60 (33)
30	*Y*	242 (57)	212 (42)	290 (78)	33 (9)	14 (4)	46 (14)	0 (5)	0 (129)	117 (32)
31	*M*	325 (71)	222 (69)	333 (107)	12 (3)	12 (4)	71 (18)	0 (1)	0 (17)	190 (39)
32	*M*	172 (81)	78 (36)	264 (98)	19 (5)	7 (2)	20 (20)	0 (1)	0 (17)	−40 (41)
33	*M*	473 (118)	186 (80)	245 (155)	39 (10)	16 (4)	88 (34)	0 (1)	0 (17)	359 (58)
34	*O*	243 (77)	167 (35)	213 (94)	12 (3)	18 (5)	53 (22)	0 (2)	0 (22)	168 (41)
35	*O*	103 (36)	112 (48)	189 (64)	17 (5)	6 (2)	17 (10)	0 (2)	0 (22)	4 (23)
36	*O*	194 (84)	176 (57)	408 (110)	21 (6)	8 (2)	33 (24)	0 (2)	0 (22)	−67 (41)

Values are in grams carbon per m^2 ground basis unless indicated otherwise. Uncertainties are shown in parentheses: Uncertainty estimates were determined by using various estimates of component errors and propagating this error through the computation of each flux either arithmetically or through Monte Carlo simulation of 1000 iterations (See Methods and materials).
**I*, initiation; *Y*, young; *M*, mature; *O*, old.

NPP_A, Aboveground net primary productivity; NPP_B, Belowground net primary productivity; R_{hS}, Heterotrophic respiration in soil; R_{hCWD}, Respiration of coarse woody detritus; R_{hFWD}, Respiration of fine woody detritus; ΔC_{CR}, Net change in coarse root C pool; ΔC_{FR}, Net change in fine root C pool; ΔC_S, Net change in soil C pool; NEP, Net ecosystem productivity.

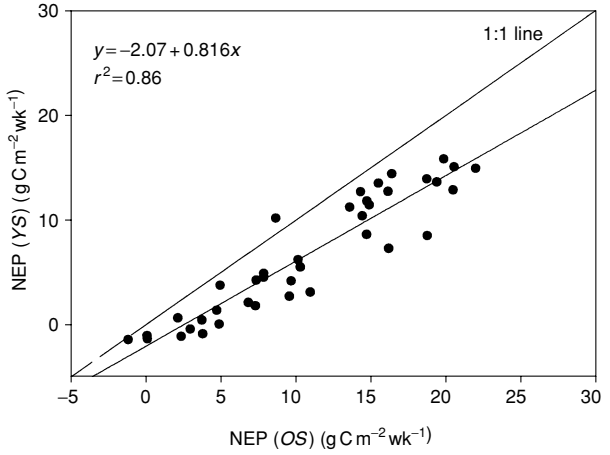

Fig. 1 Weekly net ecosystem productivity (NEP) from micrometeorological measurements made at the old pine flux site (*OS*) and initiation pine flux site (*YS*).

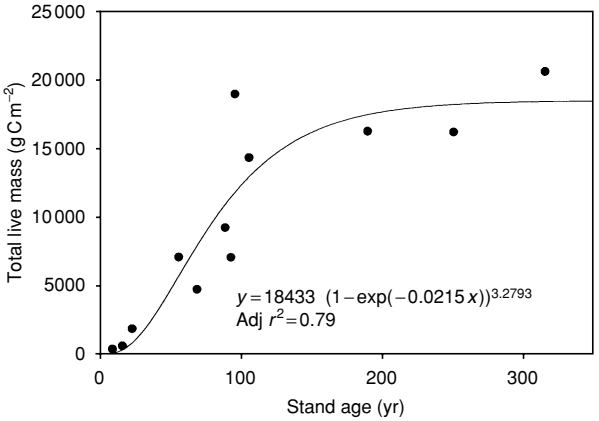

Fig. 3 Total live biomass (above and belowground) of ponderosa pine stands as a function of stand age in the Metolius area of central Oregon.

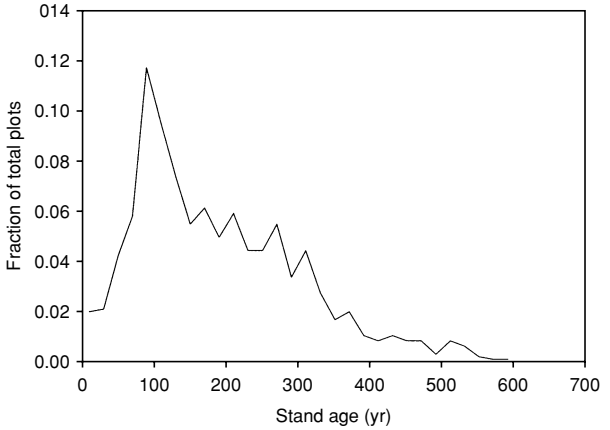

Fig. 2 Frequency distribution of ponderosa pine on federal (CVS survey plots) and private (FIA survey plots) lands in Oregon as of 1998, representing stands where 80% or more of the trees are ponderosa pine.

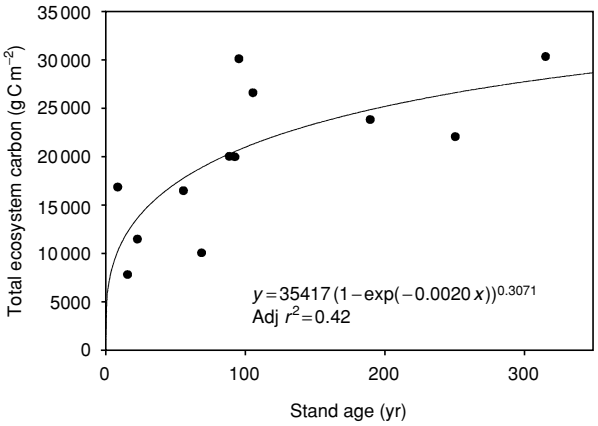

Fig. 4 Total ecosystem carbon, including live and dead carbon pools and soil C, of ponderosa pine stands in the Metolius area of central Oregon.

Chronosequence carbon balances

Carbon storage in live mass increased to a maximum of 17.6 kg C m^{-2} by approximately age 200, and did not decline thereafter (Fig. 3, Table 3). Similar patterns were observed in bolewood carbon in *Pseudotsuga menziesii–Tsuga heterophylla* forests, which reach a maximum at approximately 200 year after disturbance and didn't decline in the oldest stands (Janisch & Harmon, 2002). Total ecosystem carbon, which includes live and dead biomass and soil C, reached a maximum at ~200 year (Fig. 4), was significantly lower in the *I* stands, with values for the *I* stands less than half that of the *O* stands (Table 5). Aboveground wood mass (bole, branches and bark of trees) accounted for an average of 52% of total ecosystem carbon in the *O* stands, and reached a maximum at about 200 year (Fig. 5). The ratio of fine root to foliage carbon decreased exponentially with age, indicating that relatively more carbon is allocated to roots early in stand development permitting trees to access limited soil water (Fig. 6).

Heterotrophic respiration, estimated from Eqns (5) and (6), did not appear to vary with stand age, and the contribution from soil averaged 88% across sites (Fig. 7). In Law *et al*. (2001a), we estimated R_h at plots 25 and 34 by separation of autotrophic and heterotrophic contributions to soil CO_2 flux and R_{hWD}, and similarly found that 80–90% of R_h was from soil and fine litter.

Net ecosystem production was lowest in the *I* stands (–124 g C m^{-2} yr^{-1}), moderate in *Y* stands (118 g C m^{-2} yr^{-1}), highest in *M* stands (170 g C m^{-2} yr^{-1}), and

Table 5 Summary of carbon pools and carbon fluxes of ponderosa pine stands by age classes in the Metolius area of central Oregon

Mean age, class	Total LAI*	LM_A†	LM_B‡	Fine litter C§	Ecosystem C¶	NPP**	NEP††
20, *I*	0.71 (0.68) b	626 (213) b	283 (277) c	1230 (433) b	12 055 (4547) b	208 (87) b	−124 (106) b
70, *Y*	2.30 (0.71) a	5271 (1623) b	1685 (630) bc	994 (226) b	15 513 (5051) b	400 (48) ab	118 (59) ab
100, *M*	2.82 (0.76) a	10 173 (4432) a	3251 (1543) ab	1981 (157) a	25 603 (5143) a	485 (212) a	170 (200) a
250, *O*	2.12 (0.34) a	13 420 (1981) a	4187 (542) a	1425 (459) ab	25 423 (4348) a	332 (103) ab	35 (120) ab

Standard deviations are shown in parentheses.
Values designated by the same letters are not significantly different at $P < 0.05$ ($n = 3$).
*LAI calculated as m^2 half-surface area foliage per m^2 ground, and corrected for clumping and wood interception.
†LM_A is aboveground live mass, including understorey woody and herbaceous plants, in g C m^{-2} ground area.
‡LM_B is belowground live mass, in g C m^{-2} ground area.
§Forest floor fine litters, in g C m^{-2} ground area.
¶Ecosystem C is the sum of live and dead carbon pools and soil carbon, in g C m^{-2} ground area.
**Total net primary productivity in g C m^{-2} yr^{-1}.
††Net ecosystem productivity in g C m^{-2} yr^{-1}.

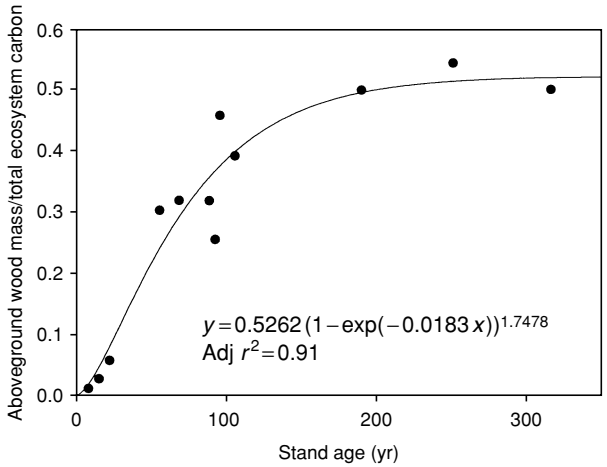

Fig. 5 Ratio of aboveground wood mass to total ecosystem carbon reaches an asymptote at about stand age 100 year in ponderosa pine stands in the Metolius area of central Oregon.

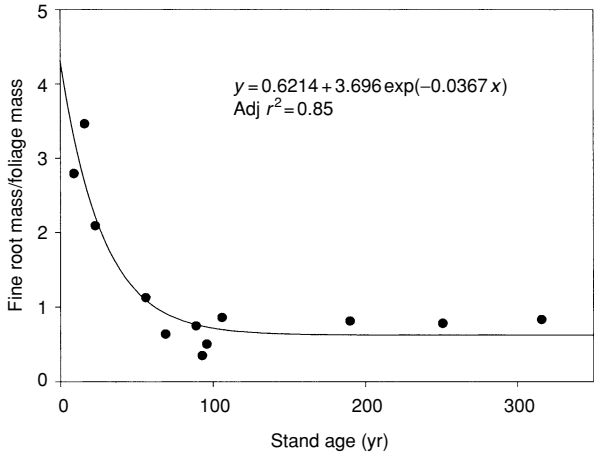

Fig. 6 Ratio of fine root mass to foliage mass as a function of stand age, indicating a change in carbon allocation patterns with stand developmental stage in ponderosa pine stands in the Metolius area of central Oregon.

low in the *O* stands (35 g C m^{-2} yr^{-1}) (Fig. 8, Tables 4 and 5). The mean NEP of the 12 stands was 50 ± 160 g C m^{-2} yr^{-1}. The variation in NEP of the *M* stands was high because one stand had been thinned about 10 year previously and another stand includes very productive grand fir (33% difference in NPP_A and 54% difference in R_S between the stands with the lowest and highest NEP values in the *M* stand age class). Such structural and compositional heterogeneity is typical for mature stands in this region. Statistically, the only significant differences in NEP were between *I* and *M* stands; NEP values of the *M* stands were significantly higher than the *I* stands. The *O* stands, ranging from 190 to 316 year were mostly a net sink for atmospheric CO_2, albeit a much weaker sink than *M* stands (Table 4). Binkley *et al*. (2002) hypothesized that differentiation in stand structure, as is commonly observed in old forests, leads to an overall decrease in wood production per unit resource used because non-dominant trees may decrease total ecosystem growth due to lower resource acquisition and resource-use efficiency than the dominant trees. On the other hand, canopy gaps form in old forests due to a variety of small-scale disturbances, allowing dense patches of trees to develop. At the *OS* flux site, NPP_A of a 50-year-old-stand (225 g C m^{-2} yr^{-1}) was greater than that of a mixed age stand (126 g C m^{-2} yr^{-1}), and the lowest NPP_A was observed in a pure old stand (96 g C m^{-2} yr^{-1}) which also had the lowest stand density (Law *et al*., 2001b). Pure stands of old ponderosa pine trees in eastern Oregon are typically small patches (e.g. 1–2 ha), thus at the spatial scale of flux measurements, the complex structure of the old forest may lead to greater net carbon uptake than

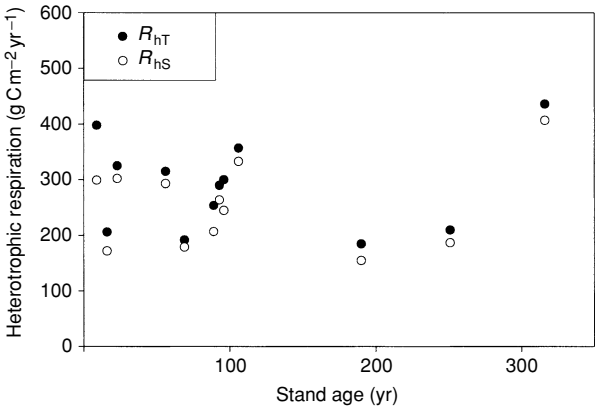

Fig. 7 Total heterotrophic respiration (R_{hT}) and heterotrophic respiration from soil (R_{hS}) of ponderosa pine stands in the Metolius area of central Oregon.

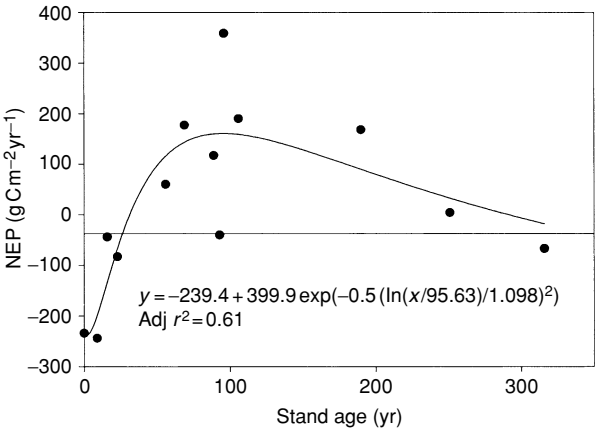

Fig. 8 Net ecosystem production (NEP) as function of stand age in ponderosa pine stands in the Metolius area of central Oregon.

would be expected from models based on homogenous stands.

Net primary production followed generally the similar trends as NEP, but did not decline as much in the *O* stands (Table 5) which was driven mainly by the trends of NPP_A (Table 4). Belowground net primary production was low in the *I* stands (averaged 94 ± 53 g C m^{-2} yr^{-1}), and high in other three stand age classes that did not differ from each other (averaged between 169 ± 47 g C m^{-2} yr^{-1} in *Y* stands and 152 ± 35 g C m^{-2} yr^{-1} in *O* stands).

Forest inventory data from the Forest Inventory Analysis (FIA) and Current Vegetation Survey (CVS) in Oregon provided age distributions for 5400 plots, 950 of which had 80% or more ponderosa pine trees (probability-based designs). The greatest proportion of plots is in the 90–130 year age classes (Fig. 2). A curve fitted to our NEP data and scaled according to proportion of total survey plots in each age class results in a mean net sink of about 70 g C m^{-2} yr^{-1}. This is a relatively low value compared with other temperate coniferous forests, but reasonable for a semiarid region. For example, annual NEP at flux sites in coniferous forests in Howland Maine and Duke Forest North Carolina averaged 250 and 595 g C m^{-2} yr^{-1}, respectively (Hollinger *et al*., 1999; Law *et al*., 2002). Flux studies in 15 European forests show a large range in NEP, from a net source of 100 to a sink of 660 g C m^{-2} yr^{-1} across forest types and latitudes (Valentini *et al*., 2000). Disturbance effects were attributed to some of this variation (e.g. high respiration in a Swedish forest that is losing carbon because of past soil drainage).

Modeling

One of the most significant model biases reported in Law *et al*. (2001b) for simulations at a subset of these sites was an overestimation of fine root biomass, and new observations from this study helped to confirm that result. On this basis, we concluded that the model treatment of fine root phenology was likely flawed, and we altered it as follows. The previous model version (Biome-BGC v 4.1.1, Thornton *et al*., 2002) forced the annual turnover rate for fine roots and leaves to be the same, so in evergreen vegetation the fine roots persisted for more than one year. Observations of fine root biomass and production from this study show that the fine root lifespan is much shorter than that for foliage, being approximately one year compared to an average of about four years for foliage. The effect of this change in the model is to reduce the standing fine root biomass and the associated maintenance respiration costs, increasing productivity. Prior to this change we found it impossible to simulate the large ratios of fine root production to foliage production observed in the young stands – the model would predict unreasonably low leaf area due to high maintenance respiration costs.

Preliminary model simulations using fixed allocation ratios showed that the accumulation of woody biomass was too slow and that the ratios of fine root mass to foliage mass for young stands were too low, compared to observations. Based on the observed annual production of wood and fine root vs. foliage across the chronosequence, we established two simple linear relationships that forced the wood and fine root allocation ratios to start at relatively high values and decrease with time since disturbance, remaining at a constant value after 150 year. The allocation ratio for aboveground wood production : leaf production was set to vary from 6 : 1 to 2 : 1, and the allocation ratio for fine root production : leaf production from 7 : 1 to 3 : 1.

We found that high allocation to both fine roots and wood relative to foliage in the young stands caused the model to significantly under-predict the rate of increase

in leaf area over time, resulting in low productivity for older stands when compared to observations, so we explored the possibility that per-unit-leaf area photosynthetic potential, held constant in the default model parameterization, was in fact varying with stand age. There was no trend in measured foliar C : N with stand age, suggesting that increases in mass-based N concentration could not be invoked to produce variation in area-based photosynthetic rates (Fig. 9). Similarly, there was no trend in canopy average specific leaf area (SLA) with stand age, suggesting that increases in area-based N concentration could also not be invoked to produce this variation (Fig. 9). Analysis of A–C_i curves collected for fully developed leaves from 15- and 50-year-old-trees at two of the chronosequence stands (plots 25 and 34) showed a decrease in the apparent fraction of leaf nitrogen in the Rubisco enzyme (*flnr*) with tree age (Table 6). We refer to *flnr* as an apparent fraction since variation between stands in specific activity of Rubisco and/or actual fractional allocation of leaf nitrogen to Rubisco could cause variation in A–C_i responses. We implemented a linear decrease in *flnr* with age, varying from 0.12 to 0.04 for stand ages from 0 to 150 years, and constant at 0.04 thereafter. This represents a new hypothesis that we were able to define and explore through simulations, but which remains to be thoroughly tested against additional observations.

To summarize, the final model parameterization included modifications to the previously described version as follows: (1) fine root lifespan set to 1 year, independent of the leaf lifespan; (2) wood and fine root allocation varying with stand age; (3) *flnr* decreasing with stand age.

The simulated variation in the ratio of fine root mass to foliage mass was consistent with observations over the entire chronosequence (Fig. 10). Observations were made for both fine and small roots, covering a range in root size up to 2 cm in diameter, and the model results agreed more closely with the measurements for the fine root class than the small root class. Simply assuming the lifespan for fine roots is shorter than that for foliage produces a pattern similar to that shown in Figs 6 and 10, because the fine root mass reaches a steady state value sooner than the foliage mass, but this mechanism alone can explain only about half of the observed variation in mass ratio with stand age. Decreasing fine root allocation with age was required to simulate the full amplitude of the change in the mass ratio. Compared to the default model parameterization, which kept the fine root allocation constant at its mature value, this has the effect of delaying the period of rapid leaf area development by

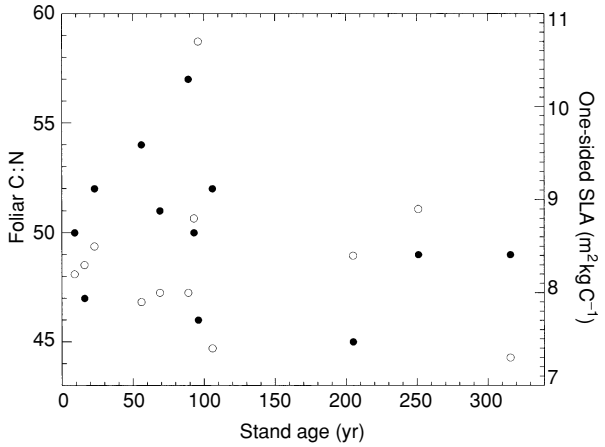

Fig. 9 Foliar C : N (●) and one-sided specific leaf area (○) as functions of stand age in ponderosa pine stands in the Metolius area of central Oregon. No significant trend for either relationship.

Table 6 Summary of analysis of A–C_i curves to estimate *flnr* in two age classes

Age	Yearday	Trees (curves)*	T range† min	T range† max	SLA‡ ($m^2 kg^{-1} C$)	Foliar C : N	V_{cmax} (25 °C)§ ($\mu mol\, m^{-2} s^{-1}$)	*flnr*	MAE¶ ($\mu mol\, m^{-2} s^{-1}$)	Bias¶ ($\mu mol\, m^{-2} s^{-1}$)
15	155	4 (5)	10.9	20.5	8.4	50	76.7	0.075	1.4	+0.6
15	232	3 (6)	12.4	26.3	8.4	50	76.7	0.075	1.7	+0.7
50	153	4 (7)	12.3	19.6	8.4	53	43.4	0.045	1.6	−0.3
50	231	4 (7)	10.2	29.1	8.4	53	53.1	0.055	2.1	+1.6

*Number of trees sampled and A–C_i curves collected at each site on each date.

†Range in measured leaf temperature during A–C_i curve collection.

‡One-sided specific leaf area.

§Corresponding to the fitted values for *flnr*, measured values for SLA and foliar C : N, and values for Rubisco activity (at 25 °C) and mass fraction of nitrogen in the Rubisco molecule as given in the text.

¶Mean absolute error (MAE) and bias in fitted model estimate of assimilation across all A–C_i points collected at a given site on a given date.

about 5 year, also delaying the peaks in GPP, NPP, and NEP.

The simulated leaf area over the chronosequence agrees well with observations for young and old stands, but is significantly lower than observed for several stands with ages around 100 year (Fig. 11). These results highlight the difficulty in inferring time trajectories from the chronosequence – variations in species mixtures, ground water availability, and management practices between stands are likely to play an important role in the observed differences, none of which have been included in the simulations.

The modeled and observed patterns of net carbon exchange are similar, in that both show an early source, followed by a strong sink that declines with age, approaching neutral carbon status for the oldest stands (Fig. 12). The modeled and observed peak sink strengths are similar, but the model predicts a more rapid shift from source to sink during the early stages of stand development following disturbance, with the modeled peak sink strength occurring around stand age 25 year, compared to the observed peak around 70–100 year. A possible explanation for this bias is that during this period the trees are competing with established shrubby and herbaceous vegetation for water and nutrient resources, an effect not accounted for in the model. These results suggest that an accurate representation of early recovery dynamics in this system might require a more sophisticated model that can explicitly represent competition between multiple plant functional types (Bachelet *et al*., 2001).

The variation in total ecosystem carbon (the year-to-year integral of NEP) agrees well with observations across the chronosequence (Fig. 13), although there is a tendency for accumulation of live mass to be too rapid during the first 50–100 year (Fig. 14), consistent with the overestimation of NEP during this period. Comparing the simulated and observed NEP for the two oldest stands (plots 35 and 36), it appears that the two-layer canopy (and two distinct age classes) for plot 36 is responsible for it having a higher NEP.

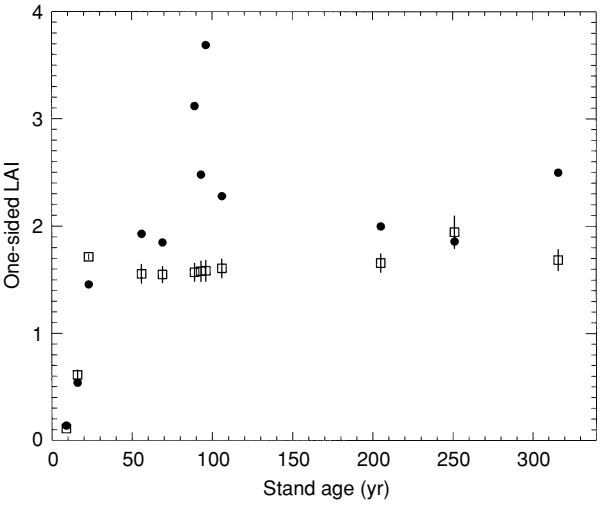

Fig. 11 Simulated one-sided leaf area index (LAI) as a function of stand age (squares, vertical bars show one standard deviation range of climate-driven interannual variability) and observed overstorey LAI (●).

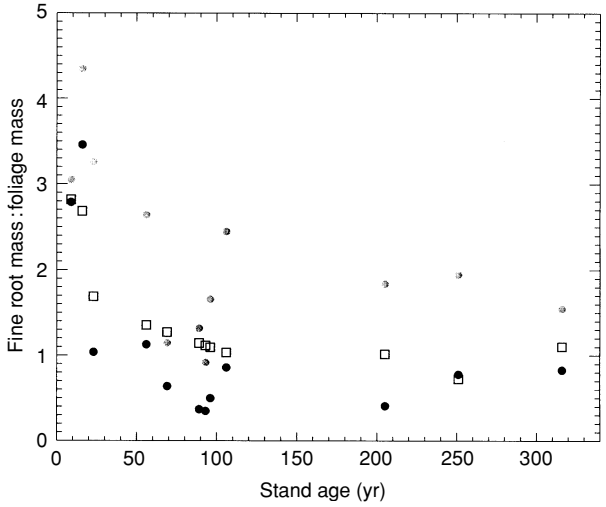

Fig. 10 Simulated ratio of fine root mass to foliage mass as a function of stand age (□) and observed ratios for two different root size classes: fine roots (< 2 mm diameter, black circles), and small roots (2 mm–2 cm diameter, grey circles).

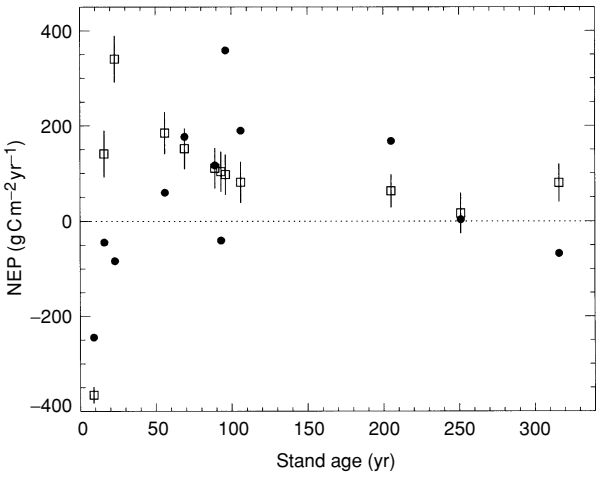

Fig. 12 Simulated net ecosystem production (NEP) as a function of stand age (squares, vertical bars show one standard deviation range of climate-driven interannual variability), and observed NEP (●).

The simulated response in NEP during the first 100 year following disturbance had a strong dependence on the atmospheric concentration of CO_2, which varied according to the historical timing of disturbances at different stands in the chronosequence. The peak carbon sink strength was higher and occurred sooner following disturbance for the more recently disturbed stands. The time required to replace the carbon lost as a result of disturbance was shorter in these stands, and the total carbon lost before the stands switched from sources to sinks of carbon was less, consistent with previous simulation results (Law *et al*., 2001b; Thornton *et al*., 2002). The CO_2 effect interacts strongly with the variation in available soil mineral nitrogen, which increases after disturbance due to reduced plant demand. The simulated NEP response to increasing atmospheric CO_2 in the oldest undisturbed stand (plot 35) is very small and is proportional to the rate of change in CO_2 concentration, rather than its absolute value, as noted previously for old stands in general (Thornton *et al*., 2002).

A combination of biological measurements and eddy covariance flux estimates from these sites has enabled a thorough evaluation of the Biome-BGC model, in this and two previous studies. These evaluations revealed several aspects of the model's logic that were too simple to accurately capture age-dependent variations in NEP. The observations also suggest new parameterizations that have improved our ability to simultaneously estimate carbon pools and fluxes in this system. These modifications now stand as new hypotheses to be tested for generality in other systems and with additional types of observations.

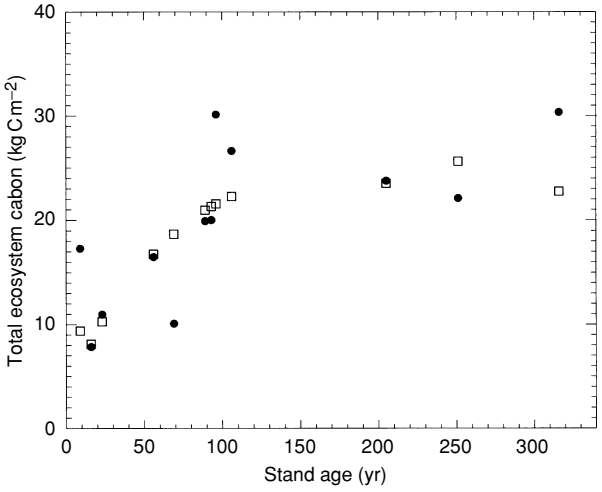

Fig. 13 Simulated total ecosystem carbon as a function of stand age (□), and observed values (●).

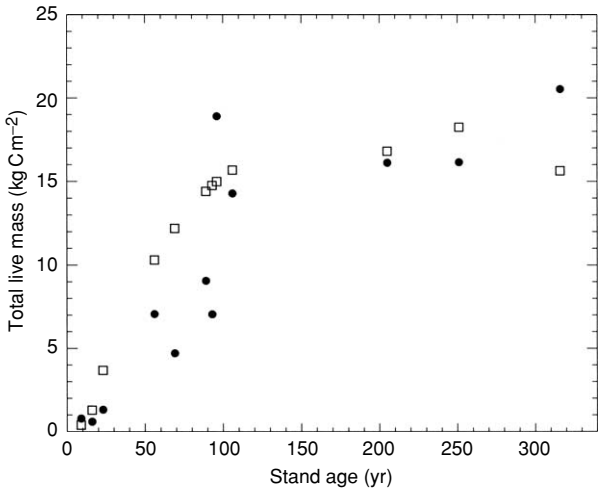

Fig. 14 Simulated total live mass as a function of stand age (□), and observed values (●).

Conclusions

Net primary production, heterotrophic respiration, and NEP were low in *I* stands, and increased to a maximum at 150–200 year, and were moderate or low in the *O* stands. The ratio of fine root to foliage carbon was highest in *I* stands, which is likely necessary for establishment in the semiarid environment, where forests are subject to drought during the growing season. Total ecosystem carbon storage and the fraction of ecosystem carbon in aboveground live wood mass increased rapidly until a stand age of 150–200 year, but did not decline in older stands. Forest inventory data on 950 ponderosa pine plots on federal (CVS) and private land (FIA) in Oregon show that the greatest proportion of plots exist in stands ~100 year old, suggesting a majority of stands are approaching maximum carbon storage and net carbon uptake. We estimate that NEP averages ~70 g C m^{-2} yr^{-1} for ponderosa pine forests in Oregon based on the age class distribution in the survey data. About 85% of the total carbon storage in biomass on the survey plots exists in stands greater than 100 year, which has implications for managing forests for carbon. Historically, rotation age for ponderosa pine has been 80–120 year if the objective was wood production (Brian Tandy, Silviculturist of Sisters Ranger District, pers. comm.). If this were still the case, we would expect a large decline in carbon storage in live biomass from logging in the near future. However, recent changes in management have been towards thinning regimes that remove the undergrowth to accelerate development of late successional habitat and to reduce fire hazard. This may moderately reduce carbon storage in biomass, but it could change carbon dynamics such that the ponderosa pine region of Oregon could on

average become a net source for CO_2, because of lower NPP but relatively small changes in heterotrophic respiration from soil. Accurate simulation of these dynamics requires a dynamic parameterization for biomass allocation that depends on stand age, and should also include a representation of competition between multiple plant functional types for space, water, and nutrients.

Acknowledgements

This study was funded by US EPA National Center for Environmental Research (NCER) Science to Achieve Results (STAR) Program (Grant # R-82830901-0), and NASA (grant # NAG 5-11231), DOE (Grant # FG0300ER63014). Funding for model evaluation was provided by NASA's Carbon Cycle Science Program (Grant # W-19953). Additional support for P. E. Thornton was provided by the National Center for Atmospheric Research (NCAR). National Center for Atmospheric Research is sponsored by the National Science Foundation. We gratefully acknowledge the Sisters Ranger District of the US Forest Service for permission and assistance to access to the study sites. We thank Mark Harmon and Jay Sexton for help and useful discussion on sampling coarse and fine woody detritus, and Darrin Moore for assisting sample collections. Acknowledgements of field sampling and data collection and root sample processing to: Jesse Bablove, Jason Barker, Aaron Domingues, David Dreher, Marie Ducharme, Isaac Emery, Nathan Gehres, Angie Hofhine, Erica Lyman-Holt, Adam Pfleeger, Lucia Reithmaier, Matthew Shepherd, Nathan Strauss, Vernon Wolf.

References

Amiro BD (2001) Paired-tower measurements of carbon and energy fluxes following disturbance in the boreal forest. *Gobal Change Biology*, **7**, 253–268.

Anthoni PM, Unsworth MH, Law BE *et al.* (2002) Seasonal differences in carbon and water vapor exchange in young- and old-growth ponderosa pine ecosystems. *Agricultural and Forest Meteorology*, **111**, 203–222.

Bachelet D, Lenihan JM, Daly C *et al.* (2001) MC1: A dynamic vegetation model for estimating the distribution of vegetation and associated ecosystem fluxes of carbon, nutrients, and water. USDA Forest Service General Technical Report PNW-GTR-508.

Barrett JW (1979) Silviculture of ponderosa pine in the Pacific Northwest: the state of our knowledge. USDA Forest Service General Technical Report PNW-97.

Binkley D, Stape JL, Ryan MG *et al.* (2002) Age-related decline in forest ecosystem growth: an individual tree, stand-structure hypothesis. *Ecosystems*, **5**, 58–67.

Brooks JR, Meinzer FC, Coulombe R *et al.* (2002) Hydraulic redistribution of soil water during summer drought in two contrasting Pacific Northwest coniferous forests. *Tree Physiology*, **22**, 1107–1117.

Cohen WB, Harmon ME, Wallin DO *et al.* (1996) Two decades of carbon flux from forests of the Pacific Northwest. *Bioscience*, **46**, 836–844.

Cooper CF (1960) Changes in vegetation, structure, and growth of southwestern pine forests since while settlement. *Ecological Monographs*, **30**, 129–164.

Giardina CP, Ryan MG (2002) Total belowground carbon allocation in a fast-growing *Eucalyptus* plantation estimated using a carbon balance approach. *Ecosystems*, **5**, 487–499.

Harmon ME, Ferrell WK, Franklin JF (1990) Effects on carbon storage of conversion of old-growth forests to young forests. *Science*, **247**, 699–702.

Harmon ME, Sexton J (1996) *Guidelines for Measurements of Woody Detritus in Forest Ecosystems. Publication No. 20.* US LTER Network Office, University of Washington, Seattle, WA.

Hollinger DY, Goltz SM, Davidson EA *et al.* (1999) Seasonal patterns and environmental control of carbon dioxide and water vapour exchange in an ecotonal boreal forest. *Global Change Biology*, **5**, 891–902.

IPCC (2001) Climate Change 2001: Synthesis Report (eds Watson R T, The Core Writing Team), Geneva, Switzerland, pp. 184. (http://www.ipcc.ch).

Irvine J, Law BE, Anthoni PM *et al.* (2002) Water limitations to carbon exchange in old-growth and young ponderosa pine stands. *Tree Physiology*, **22**, 189–196.

Janisch JE, Harmon ME (2002) Successional changes in live and dead wood carbon stores: impolications for net ecosystem productivity. *Tree Physiology*, **22**, 77–89.

Kuehn GD, McFadden BA (1969) Ribulose 1,5-diphosphate carboxylase from *Hydrogenomonas eutropha* and *Hydrogenomonas facilis*. II. Molecular weight, subunits, composition, and sulfhydryl groups. *Biochemistry*, **24**, 359–371.

Law BE, Falge E, Baldocchi DD *et al.* (2002) Environmental controls over carbon dioxide and water vapor exchange of terrestrial vegetation. *Agricultural and Forest Meteorology*, **113**, 97–120.

Law BE, Kelliher FM, Baldocchi DD *et al.* (2001a) Spatial and temporal variation in respiration in a young ponderosa pine forest during a summer drought. *Agricultural and Forest Meteorology*, **110**, 27–43.

Law BE, Thornton P, Irvine J *et al.* (2001b) Carbon storage and fluxes in ponderosa pine forests at different developmental stages. *Global Change Biology*, **7**, 755–777.

Law BE, van Tuyl S, Cescatti A *et al.* (2001c) Estimation of leaf area index in open-canopy ponderosa pine forests at different successional stages and management regimes in Oregon. *Agricultural and Forest Meteorology*, **108**, 1–14.

Litvak M, Miller S, Wofsy FC *et al.* (2003) Effect of stand age on whole ecosystem CO_2 exchange in the Canadian boreal forest. *Journal of Geophysical Research*, **108**.

Monleon VJ, Cromack K, Landsberg J (1997) Short and long-term effects of prescribed underburning on nitrogen availability in ponderosa pine stands in Central Oregon. *Canadian Journal of Forest Research*, **27**, 369–378.

Raich JW, Nadelhoffer KJ (1989) Belowground carbon allocation in forest ecosystems: global trends. *Ecology*, **70**, 1346–1354.

Riegel GM, Miller RF, Krueger WC (1992) Competition for resources between understorey vegetation and overstorey Pinus ponderosa in northeastern Oregon. *Ecological Applications*, **2**, 71–85.

SAS Institute Inc. (1999) SAS OnlineDoc, Version 8. Cary, NC, USA.

Schimel DS, House JI, Hibbard KA *et al.* (2001) Recent patterns and mechanisms of carbon exchange by terrestrial ecosystems. *Nature*, **414**, 169–172.

Thornton PE, Hasenauer H, White MA (2000) Simultaneous estimation of daily solar radiation and humidity from observed temperature and precipitation: an application over complex terrain in Austria. *Agricultural and Forest Meteorology*, **104**, 255–271.

Thornton PE, Law BE, Gholz HL *et al.* (2002) Modeling and measuring the effects of disturbance history and climate on carbon and water budgets in evergreen needleleaf forests. *Agricultural and Forest Meteorology*, **113**, 185–222.

Thornton PE, Running SW (1999) An improved algorithm for estimating incident daily solar radiation from measurements of temperature, humidity, and precipitation. *Agricultural and Forest Meteorology*, **93**, 211–228.

Thornton PE, Running SW, White MA (1997) Generating surfaces of daily meteorological variables over large regions of complex terrain. *Journal of Hydrology*, **190**, 214–251.

Valentini R, Matteucci G, Dolman AJ *et al.* (2000) Respiration as the main determinant of carbon balance in European forests. *Nature*, **404**, 861–865.

Wilson KB, Baldocchi DD, Hanson PJ (2000) Spatial and seasonal variability of photosynthetic parameters and their relationship to leaf nitrogen in a deciduous forest. *Tree Physiology*, **20**, 565–578.

Woodrow IE, Berry JA (1988) Enzymatic regulation of photosynthetic CO_2 fixation in C_3 plants. *Annual Reviews of Plant Physiology and Plant Molecular Biology*, **39**, 533–594.